Binding of a Photoaffinity Analogue of Glutathione to MRP1 (ABCC1) within Two Cytoplasmic Regions (L0 and L1) as Well as Transmembrane Domains 10-11 and 16-17†

Joel Karwatsky,‡ Roni Daoud,‡ Jie Cai,§ Philippe Gros,§ and Elias Georges*,‡

Institute of Parasitology and Department of Biochemistry, McGill University, Quebec, Canada

Received September 20, 2002; Revised Manuscript Received December 21, 2002

ABSTRACT: MRP1 (or ABCC1) is an ABC membrane protein that transports a wide range of natural products as well as glutathione (GSH)-, glucuronate-, and sulfate-conjugated metabolites. In addition, free GSH is required for MRP1 to transport several chemotherapeutic drugs. However, the mechanisms regulating the influence of GSH on MRP1 is poorly understood, and the location of GSH binding site(s) within MRP1 have yet to be determined. To address these issues, we have synthesized a [^{125}I] labeled azido-derivative of GSH (IAAGSH) to photoaffinity label MRP1. Our results revealed that IAAGSH labeled MRP1 with high specificity, and binding was inhibited by MRP1 substrates leukotriene C_4 and MK571. Interestingly, verapamil and vincristine enhanced IAAGSH photolabeling of MRP1, in agreement with observations that both drugs enhance GSH transport. We observed GSH to be the best inhibitor of photoaffinity labeling, as compared to oxidized glutathione (GSSG) and four different GSH alkyl derivatives. These observations indicate that IAAGSH interacted with MRP1 in a similar manner as unmodified GSH. Moreover, using eight MRP1-HA variants, each containing hemagglutinin A (HA) epitopes inserted at different sites in MRP1, we mapped the GSH binding sites in MRP1. Our GSH analogue photoaffinity labeled four MRP1 polypeptides that were located within two cytoplasmic domains in linker sequences (L0 and L1) as well as transmembrane domains 10-11 and 16-17. The photoaffinity labeling of polypeptides within L0 and L1 domains is further confirmed using two MRP1-specific monoclonal antibodies (MRPr1 and QCRL1) with epitopes within the linker domains. Taken together, this study provides the most precise information to date on the location of GSH binding sites in MRP1.

Several types of cancer respond to initial drug treatment but develop resistance upon further therapy (e.g., lymphoma and breast cancer) (*1*). The emergence of drug resistance usually prevents treatment from being curative. A more critical problem arises when cancers develop multidrug resistance (MDR),[1] which is characterized by a resistance to a diverse group of chemically unrelated drugs. In vitro selection of tumor cell lines for resistance to anticancer drugs causes the overexpression of large integral membrane proteins such as P-glycoprotein 1 (P-gp1) or the multidrug resistance protein 1 (MRP1 or ABCC1) (*2, 3*). Both P-gp1 and MRP1 function as broad-specificity drug pumps that bind and transport drugs against a concentration gradient using ATP hydrolysis as an energy source (*4, 5*).

P-gp1 and MRP1 are both members of the ATP-binding cassette (ABC) superfamily of transport proteins. Although they share only 15% amino acid identity (*3*), both P-gp1 and MRP1 confer resistance to many natural product anticancer drugs including methotrexate, epipodophyllotoxins, vinca alkaloids, and certain anthracyclines (*6*−*8*). Despite their similar resistance profiles, several key differences exist. Unlike P-gp1, the preferred substrates of MRP1 are organic anions, including drugs conjugated to glutathione, sulfate, or glucuronate (*9*−*12*). In addition, considerable evidence indicates that GSH is required for MRP1 to transport unmodified drugs such as vincristine and daunorubicin (*13*−*15*). GSH may also be co-transported with some of these compounds (*16*). Potential physiological substrates of MRP1 may include glucuronidate- and sulfate-conjugated bile salts, oxidized glutathione (GSSG), as well as the GSH conjugates leukotriene C_4 (LTC_4) and prostaglandin A_2 (*9, 11, 12, 17*). In contrast, these conjugated organic anions are poor substrates for P-gp1.

Typically, members of the ABC superfamily are made up of one or more core regions. Each core region contains six transmembrane α-helices comprising a membrane-spanning domain (MSD) and a nucleotide-binding domain (NBD). P-gp1 contains two such core regions connected by an intracellular linker domain, with both the NH_2 and the COOH termini located in the cytoplasm (*18*, *19*). The topology of MRP1 is similar to P-gp1, although it has an additional modification at the N-terminal. MRP1 has a group of five transmembrane sequences at its N-terminal (MSD0) con-

† This work was supported by the Canadian Institute of Health Research (CIHR) and the Natural Sciences and Engineering Research Council (NSERC) (E.G.), as well as the National Cancer Institute of Canada (P.G.). A salary award from CIHR supports P.G.

* To whom correspondence should be addressed. Tel.: (514) 398-8137. Fax: (514) 398-7857. E-mail: Elias.Georges@McGill.CA.

‡ Institute of Parasitology.

§ Department of Biochemistry.

[1] Abbreviations: MDR, multidrug resistance; P-gp, P-glycoprotein; MRP, multidrug resistance protein; SDS−PAGE, sodium dodecyl sulfate polyacrylamide gel electrophoresis; ABC, ATP-binding cassette; GSH, glutathione; IAAGSH, iodoaryl azido-glutathione; hemagglutinin A, HA; monoclonal antibody, mAb.

10.1021/bi0268807 CCC: $25.00
Published on Web 02/26/2003

nected through an intracellular linker domain (L0) to a P-gp1-like core. Therefore, the predicted topological organization of MRP1 is MSD0-L0-MSD1-NBD1-L1-MSD2-NBD2 (*20*, *21*).

Several MRP1-specific photoreactive drugs have been used to show direct binding between MRP1 and unmodified natural product drugs (*22*−*26*). More recently, photoaffinity labeling studies have identified specific drug-binding regions in MRP1 using two iodinated azido derivatives; these include *N*-(hydrocinchonidin-8′-yl)-4-azido-2-hydroxybenzamide (IACI), a quinoline-based drug (*26*), as well as iodoaryl azido-rhodamine 123 (IAARh123)(*25*). These compounds photoaffinity label proteolytic MRP1 fragments that correspond to the putative transmembrane domains (TM) 10-11 and 16-17 (*27*). LTC_4 can also photoaffinity label sites in both the NH_2 and the COOH-halves of MRP1 (*28*); however, it is not clear if LTC_4 binds to the same regions as the azido-derivatives. None of these studies with azido-drug derivatives indicate that GSH is required for MRP1-drug interactions. However, GSH was shown to be required for MRP1 photoaffinity labeling with an azido-derivative of agosterol-A (*29*).

Unlike most MRP1 substrates, GSH appears to play a role in facilitating the transport process, possibly by conjugation or co-transport with other molecules. However, at present little is known about how GSH and MRP1 interact, despite the critical role GSH plays in transporting MRP1 substrates. The most familiar role of GSH in cells is as an antioxidant. GSH detoxifies reactive oxygen species by acting as a substrate for GSH transferase and GSSG reductase (*30*). In this study, we aimed to assess whether GSH interacts directly with MRP1, and if so, to identify the regions of MRP1 involved in GSH binding. To address these questions, we synthesized a radiolabeled, iodinated azido-derivative of GSH (iodoaryl-azido glutathione or IAAGSH) to photoaffinity label MRP1. Our results show that IAAGSH interacted with MRP1 specifically and at physiologically relevant sites. Furthermore, several IAAGSH binding sites were identified from photoaffinity labeled proteolytic fragments of eight MRP1 variants containing hemagglutinin A (HA) epitopes inserted at different positions (*27*, *31*, *32*). This approach has localized IAAGSH binding sites to TM 10-11 and TM 16-17, as well as to two novel cytoplasmic linker regions (L0 and L1). This information provides the most precise location of GSH binding sites within MRP1 to date.

EXPERIMENTAL PROCEDURES

Materials. Protein A Sepharose CL-4B and carrier-free Na^{125}Iodine (100 mCi/mL) were purchased from Amersham Biosciences (Baie d'Urfe, Quebec). MK571 was kindly provided by Dr. A. W. Ford-Hutchinson (Merk-Frost Centre for Therapeutic Research, Quebec (*33*)). LTC_4 was purchased from Cayman Chemical Co. (Ann Arbor, Michigan). The monoclonal anti-hemagglutinin A antibody 16B12 (anti-HA) was purchased from Berkeley Antibody Co. (Richmond, California). The QCRL1 murine hybridoma was obtained from ATCC (Nanassas, Virginia). The MRPr1 mAb was purchased from Kamiya Biomedical Company (Seattle, Washington). Trypsin (sequencing grade and TPKC treated) was procured from Roche Diagnostics (Laval, Quebec). NHS-ASA and ImmunoPure immobilized protein G were purchased from PIERCE (Rockford, Illinois). All other chemicals were of the highest possible quality.

Cell Culture and Plasma Membrane Preparation. HeLa cells were cultured in α-MEM media containing 10% fetal bovine serum (Hyclone) as previously described (*31*, *32*). HeLa cells transfected with MRP1-HA variants had a stable expression of MRP1 containing one or more copies of the HA epitope (YPYDVPDYAS) inserted after amino acids 1, 163, 271, 574, 653, 938, 1001, or 1222 from the N-terminus. For plasma membrane preparations, cells were detached with trypsin-EDTA and washed with phosphate-buffered saline, pH 7.4 (PBS). The cell pellet was then resuspended in hypotonic buffer (1 mM $MgCl_2$, 10 mM KCl, and 10 mM Tris-HCl, pH 7.4) containing protease inhibitors (2 μg/mL leupeptin, 2 μg/mL aprotinin, and 1 μg/mL pepstatin A, 1 mM PMSF). Cells were lysed in a Dounce homogenizer and centrifuged at 10 000*g* for 5 min followed by a second centrifugation at 100 000*g* for 1 h. The final pellet was resuspended in PM buffer (5 mM Tris-HCl with 250 mM sucrose, pH 7.4) and stored at −70 °C. Protein concentrations were determined by the Lowry et al. method (*34*).

Synthesis of ASA-GSH. All reactions were carried out in the dark. The synthesis of a photoreactive analogue of GSH (aryl-azido glutathione or ASA-GSH) was done as previously described (*35*) with some modifications. Briefly, 10 mg of GSH was dissolved in 75 μL of ddH2O and diluted to 500 μL with dry dimethylformamide (DMF). NHS-ASA (5.5 mg) was dissolved in 250 μL of DMF and mixed with an equal volume of the GSH solution. Triethylamine (20 μL) was added to the latter reactants and allowed to incubate for 48 h at room temperature with rotation. The reaction was terminated, and the resulting mixture was separated on high-pressure liquid chromatography using a reverse-phase C18 column from Grace Vydac (Hesperia, CA). Separation was achieved using 0.025 M ammonium acetate, pH 5.5, and an acetonitrile mobile gradient as previously described (*35*). Purified ASA-GSH was characterized by mass spectrometry, dried, and stored at −70 °C.

Iodination of ASA-GSH. ASA-GSH (30 μg) was dissolved in 10 μL of PBS and mixed with 100 μL of 3% chloramine T prepared in buffer I (10 mM Na_2HPO_4, pH 8.5) along with 2 mCi of carrier-free Na^{125}Iodine (100 mCi/mL). The reaction proceeded for 5 min at room temperature and was stopped with 100 μL of 5% Na-metabisulfate in buffer I. The sample was then loaded on a C18 SepPak column that was previously washed with 100% methanol followed by buffer I. The column was then washed 10 times with 5-mL aliquots of buffer I to remove free iodine. IAAGSH was eluted from the column with 5 mL of 100% methanol and then dried down to 50−100 μL by aspiration with N_2. Finally, the iodinated sample was resuspended in PBS.

Photoaffinity Labeling and SDS−*PAGE.* For photoaffinity labeling, IAAGSH was added to 20−100 μg aliquots of plasma membrane in PM buffer (5 mM Tris-HCl with 250 mM sucrose, pH 7.4) and incubated at room temperature for 30 min, in the dark. Samples were further incubated on ice for 10 min followed by UV irradiation at 254 nm for 10 min, as previously described (*35*). Photoaffinity labeled samples underwent proteolytic digestion and immunoprecipitation (*36*) as described below or were directly resolved by SDS−PAGE. Protein samples were resolved on SDS−PAGE exclusively using the Fairbanks et al. system (*37*).

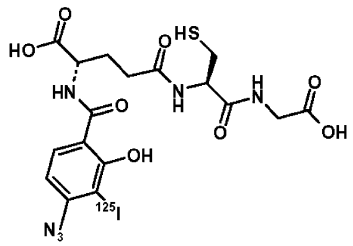

FIGURE 1: Chemical structure of radioactive iodoaryl-azido glutathione (IAAGSH).

Coomassie Blue staining was used to detect all proteins in plasma membrane samples. Alternatively, gels with radiolabeled proteins were dried and exposed on Kodak BIOMAX MS film at −80 °C.

Western Blotting. For immunodectection of P-gp1, 20 μg of enriched plasma membranes were resolved on SDS−PAGE and transferred to nitrocellulose membrane by using a wet electroblotting technique as outlined in Towbin et al. (*38*). The nitrocellulose membrane was blocked in PBS with 5% skim milk and incubated with C219 mAb overnight at 4 °C (*36*). After incubation, membranes were washed and incubated for 2 h with 1:3000 (v/v) goat anti-mouse antibody conjugated to horseradish peroxidase. SuperSignal chemoluminescent (Pierce, Rockford, IL) substrate was used to detect mAb binding.

Proteolytic Digestion and Immunoprecipitation. Photoaffinity labeled plasma membrane samples (100 μg) were digested with increasing concentrations of trypsin at 37 °C for 40 min. The digestion was stopped by placing the samples on ice and adding 80 μL of buffer A (1% SDS, 50 mM Tris-HCl, pH 7.4) with protease inhibitors (10 μg/mL leupeptin, pepstatin, aprotinin, and 1 mM PMSF). Samples were left on ice for 15 min before the addition of 320 μL of buffer B (1.25% Triton X-100, 190 mM NaCl, and 0.05 M Tris-HCl, pH 7.4). The digested peptides were immunoprecipitated as previously described (*36*). Briefly, samples were incubated overnight with protein A Sepharose beads conjugated to anti-HA or QCRL1 mAb with rotation. After incubation, samples were washed five times with buffer C (0.05% Triton X-100, 0.03% SDS, 150 mM NaCl, 5 mg/mL BSA, and 0.05 M Tris-HCl, pH 7.4) and once with buffer D (150 M NaCl and 0.05 M Tris-HCl, pH 7.4). For immunoprecipitation with MRPr1 mAb, each labeled plasma membrane sample was first pre-cleared with 50 μL of ImmunoPure immobilized protein G for 30 min and then incubated overnight with 2 μg of MRPr1 mAb. Following incubation, 50 μL of ImmunoPure immobilized protein G was added to each sample and incubated for 30 min at room temperature and 2 h at 4 °C. The samples were then washed six times with immunoprecipitation buffer (20 mM sodium phosphate, pH 7.5, 500 mM NaCl, 0.1% SDS, 1% NP-40, 0.5% sodium deoxycholate, and 0.02% sodium azide). Samples were then resolved on SDS−PAGE.

RESULTS

To investigate the interactions between MRP1 and GSH, we have synthesized a radiolabeled, photoreactive analogue of GSH, IAAGSH (Figure 1). Membrane-enriched fractions from HeLa and HeLa/MRP1 transfected cells were photoaffinity labeled with IAAGSH and resolved by SDS−PAGE (Figure 2). Lanes 1 and 2 (Figure 2A) show photoaffinity

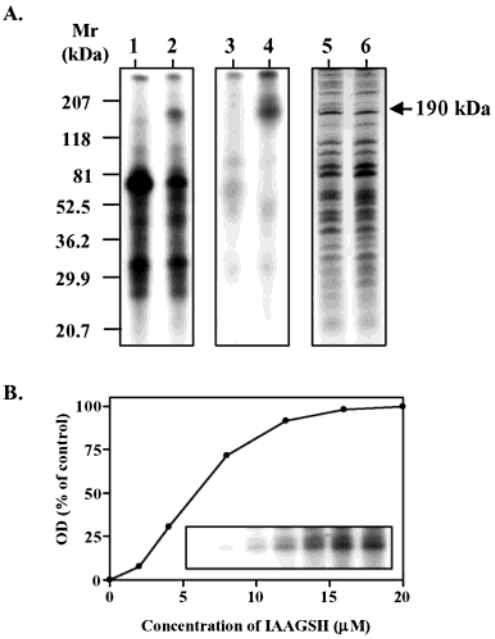

FIGURE 2: Photoaffinity labeling of HeLa and HeLa-MRP1 with IAAGSH. Plasma membranes (25−50 μg) were incubated with 0.2 μM of IAAGSH and exposed to UV light at 4 °C. Proteins from HeLa and HeLa-MRP1 were resolved on SDS−PAGE (lanes 1 and 2, respectively). Lanes 3 and 4 show an immunoprecipitation of IAAGSH photolabeled HeLa and HeLa-MRP1 membrane proteins with MRP1-specific mAb (MRPr1). Lanes 5 and 6 show the staining of membrane proteins from HeLa and HeLa-MRP1 with Coomassie Blue. The graph in panel B demonstrates the saturable photoaffinity labeling of MRP1 with increasing amounts of IAAGSH: 2, 4, 8, 12, 16, and 20 μM (seen in the inset). Lanes 1−4 of panel A and the insert in panel B are autoradiographic images.

labeling of a 190 kDa protein in membranes from HeLa/MRP1 but not HeLa cells. While multiple bands were observed, suggesting the presence of other photoaffinity labeled proteins in HeLa and HeLa/MRP1 membranes, the 190 kDa band is the only band that is selectively labeled in Hela/MRP1 transfected cells. The other labeled proteins likely represent other GSH binding proteins that interact with GSH or IAAGSH. This was not unexpected because GSH interacts with a diverse group of transferases and reductases, including glutathione *S*-transferase (*30*). To confirm the identity of the 190 kDa photoaffinity labeled protein, HeLa and HeLa/MRP1 membranes were photoaffinity labeled with IAAGSH and immunoprecipitated with MRP1-specific mAb, MRPr1, or an irrelevant IgG2a antibody. The results of Figure 2A (lanes 3 and 4) show a 190 kDa photoaffinity labeled protein immunoprecipitated from Hela/MRP1 but not from HeLa photoaffinity labeled plasma membranes. Similar immunoprecipitation with an irrelevant IgG2a did not result in the immunoprecipitation of a 190 kDa protein (data not shown). Together, the molecular mass and binding to MRPr1 mAb, as well as the results in Figure 2A (lanes 1−4), confirm the identity of the 190 kDa photolabeled protein to be MRP1. As indicated above, several other proteins from HeLa and HeLa/MRP1 enriched plasma membranes were shown to interact with IAAGSH. Consequently, it was of interest to know if the photoaffinity labeling of MRP1 in HeLa/MRP1 transfectants was exclusively because of the overexpression of MRP1 protein. To address this possibility, total membrane proteins from HeLa and Hela/MRP1 cells were resolved by SDS−PAGE and stained with Coomassie Blue. As demon-

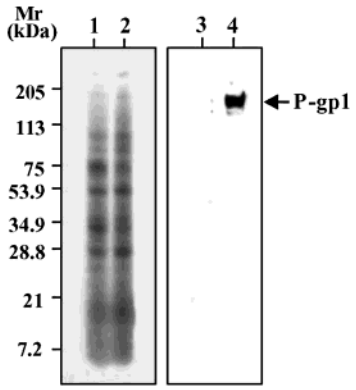

FIGURE 3: Photoaffinity labeling and Western blot of CEM and CEM/VLB1.0 membranes with IAAGSH. Plasma membranes (25−50 μg) were incubated with 0.2 μM IAAGSH and exposed to UV light at 4 °C. Proteins from CEM and P-gp1 expressing cells CEM/VLB1.0 (lanes 1 and 2, respectively) were resolved on SDS−PAGE. Lanes 3 and 4 show a Western blot of plasma membrane from the same cells (CEM and CEM/VLB1.0, respectively) with the P-gp1-specific C219 mAb.

strated in lanes 5 and 6 of Figure 2A, MRP1 is barely detectable relative to other more highly expressed proteins. Therefore, the labeling of MRP1 by IAAGSH is due to a specific interaction between the IAAGSH and the MRP1 and not because of high expression of MRP1. To demonstrate the specificity of IAAGSH toward MRP1, we examined the photoaffinity labeling of MRP1 with increasing amounts of IAAGSH (2−20 μM). Figure 2B shows that MRP1 photoaffinity labeling became saturated at 16 μM of IAAGSH. Incidentally, the band representing labeled MRP1 first appeared at 4 μM of IAAGSH, in contrast to results contained in Figure 2A showing MRP1 protein labeled with 0.2 μM of IAAGSH. However, to prevent saturation of the autoradiography film at high concentrations of IAAGSH (10−20 μM), it was necessary to reduce film exposure time for results shown in Figure 2B. Taken together, the results in Figure 2 demonstrate that IAAGSH specifically photoaffinity labeled MRP1.

To further investigate the specificity of IAAGSH toward MRP1 and to determine if P-gp1 also interacts with IAAGSH, plasma membranes from human MDR cells (CEM/VL$^{1.0}$), which overexpress P-gp1 at high levels, were photoaffinity labeled with IAAGSH. Western blot analysis with Pgp1 specific mAb (C219) confirmed high expression levels of P-gp1 in CEM/VLB$^{1.0}$ drug resistant but not in the CEM parental drug sensitive cells (lanes 3 and 4, Figure 3). Importantly, the absence of a 170 kDa band in lane 2 indicates that IAAGSH failed to interact with and photolabel P-gp1 in CEM/VLB$^{1.0}$ membranes.

Earlier studies using inside-out membrane vesicles (*16*, *39*, *40*) have indicated that GSH can modulate MRP1-mediated transport of certain anticancer drugs. Thus, it was of interest to examine the ability of known MRP1 substrates to interfere with the binding of MRP1 to IAAGSH. Figure 4 shows the effect of increasing concentrations of etoposide (VP16), MK571 (LTD_4 antagonist), doxorubicin (DOX), leukotriene C_4 (LTC_4), vincristine (VCR), and verapamil (VRP) on MRP1 binding to IAAGSH. The most effective competitors were MK571 and LTC_4. The presence of 10-fold molar excess of MK571 reduced IAAGSH photolabeling of MRP1 by more than 50%, and 100-fold excess almost

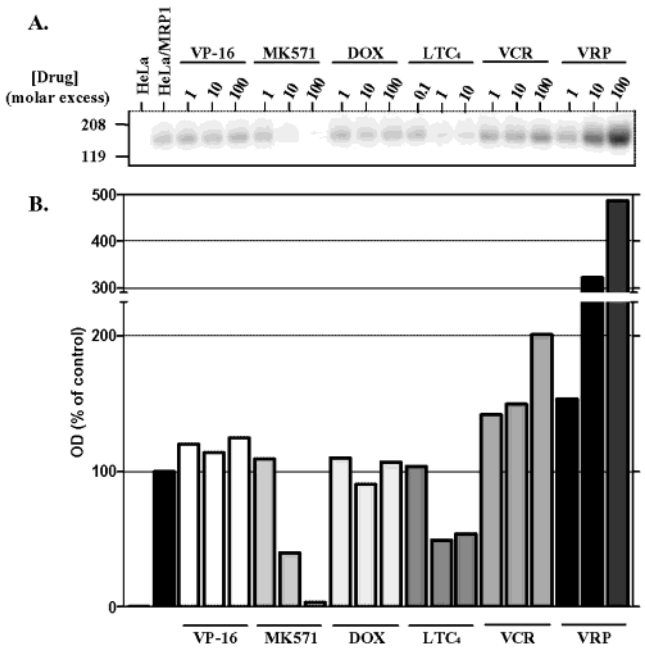

FIGURE 4: Effect of several drugs on photoaffinity labeling of MRP1 by IAAGSH. HeLa or HeLa/MRP1 plasma membranes were photoaffinity labeled with 2 μM IAAGSH in the absence or presence of etoposide (VP-16), MK571, doxorubicin (DOX), leucotriene C_4 (LTC_4), vincristine (VCR), and verapamil (VRP). LTC_4 was added in 0.1, 1, and 10 molar excess of IAAGSH. All other drugs were added in 1, 10, and 100 molar excess of IAAGSH. Panel B demonstrates the relative change in photolabeling of MRP1 with IAAGSH in the presence of the same drugs. Plasma membranes were immunoprecipitated with hemagglutinin A (HA) mAb. These results are representative of at least three individual experiments.

completely inhibited photolabeling. LTC_4 was a more potent inhibitor of IAAGSH photolabeling. It reduced IAAGSH labeling of MRP1 by approximately 50% when it was added in 1- and 10-fold molar excesses. VP-16 and doxorubicin, both substrates of MRP1, were the least effective competitors, having no significant effect even at 100-fold molar excess of IAAGSH. These results indicate that IAAGSH interacts with similar or overlapping binding sites as known MRP1 substrates. Interestingly, vincristine and verapamil enhanced the photoaffinity labeling of MRP1 by IAAGSH. Vincristine enhanced photolabeling up to about 150% of control (IAAGSH alone) at 1- and 10-fold molar excess, while at 100-fold excess vincristine more than doubled IAAGSH labeling of MRP1. Verapamil was even more effective at increasing MPR1 labeling by IAAGSH. Ten-fold molar excess of verapamil increased labeling to approximately 300% of control, and 100-fold excess increased binding to almost 500% of control.

To ascertain the binding characteristics of IAAGSH to MRP1, photoaffinity labeling of MRP1 in membranes from HeLa/MRP1 cells was conducted in the presence of increasing concentrations of reduced glutathione (GSH), oxidized glutathione (GSSG), and several alkyl-GSH derivatives: *S*-methylglutathione (Meth-GSH), *S*-ethylglutathione (Eth-GSH), *S*-hexylglutathione (Hex-GSH), and *S*-octylglutathione (Oct-GSH). The results in Figure 5 show that unmodified GSH inhibited IAAGSH labeling far more effectively than GSSG or any of the alkyl derivatives. When GSH was added at 500-fold molar excess of IAAGSH, photoaffinity labeling was completely abolished. Moreover, as little as 5-fold molar

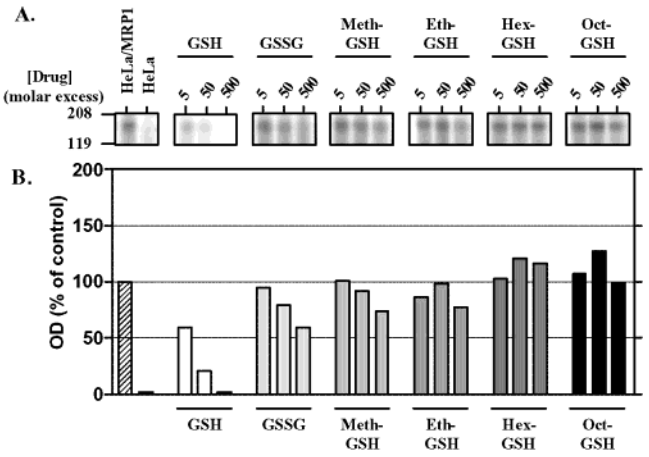

FIGURE 5: Effect of GSH and its derivatives on the photoaffinity labeling of MRP1 by IAAGSH. Panel A shows HeLa or HeLa/MRP1 plasma membranes photoaffinity labeled with 2 μM IAAGSH in the absence or presence of increasing molar excess (5, 50, and 500) of reduced glutathione (GSH), oxidized glutathione (GSSG), *S*-methylglutathione (Meth-GSH), *S*-ethylglutathione (Eth-GSH), *S*-hexylglutathione (Hex-GSH), and *S*-octylglutathione (Oct-GSH). Panel B demonstrates the relative change in photolabeling of MRP1 with IAAGSH in the presence of the same compounds. These results are representative of at least three individual experiments.

excess of GSH reduced IAAGSH labeling by half. GSSG was the next most effective inhibitor of IAAGSH photolabeling. Both methyl-GSH and ethyl-GSH caused a moderate inhibition on IAAGSH labeling relative to GSH by causing a 20−25% reduction at 500-fold molar excess (Figure 5). The two most hydrophobic GSH alkyl derivatives, hexyl-GSH and octyl-GSH, caused an increase of approximately 20 and 25%, respectively, in IAAGSH photolabeling at 50-fold molar excess. Taken together, the results of Figure 5 confirm the specificity of IAAGSH toward MRP1-GSH binding domain(s) and provide the first direct evidence for GSH and MRP1binding.

Using several variants of MRP1, we have previously identified two regions in MRP1 encoding binding sites for structurally diverse drugs. Each variant contains one or more HA epitopes inserted at eight different sites in MRP1 (Figure 6). These binding regions were localized to two peptide fragments with sizes of 6.5 and 7 kDa, encoding amino acid sequences from TM 10-11 and 16-17, respectively (*27*). Given the above results, it was of interest to determine if the binding domains of IAAGSH are the same or if they overlap these previously identified drug-binding domains. The results in Figure 6 describe the IAAGSH photoaffinity labeling of plasma membranes from each cell line transfected with the different MRP1 variants containing HA-epitopes. Each MRP1-variant was digested separately with increasing concentrations of trypsin (1:800−1:25). The digested peptide fragments were immunoprecipitated with anti-HA mAb and resolved by SDS−PAGE. The resulting polypeptide bands contained a HA epitope and a cross-linked IAAGSH.

The digestion pattern of each photoaffinity labeled MRP1 variant is displayed in Figure 6. A topological diagram of MRP1 and connecting arrows indicate the position of the inserted HA epitope in each MRP1 variant. The tryptic peptide fragments from MRP1 variant 4 (HA epitope inserted after the 4th amino acid) are visible in Figure 6A. In addition to full-length MRP1 (190 kDa), a 111 kDa fragment was resolved. This fragment corresponds to one of two peptides that results from digestion at a known trypsin-sensitive site located in the linker domain, L1 (*41*). MRP1-variants 163, 271, and 574 (Figure 6B−D, respectively) share two common peptides fragments, the previously mentioned 111 kDa band as well as a 65 kDa fragment. In addition, MRP1 variant 271 also has a photoaffinity labeled 24 kDa peptide. On the basis of its apparent molecular mass and the known trypsin cutting sites, the 24 kDa peptide is made up of approximately 216 amino acid residues and must be located somewhere between Asp_{171} (within TM 5) and Lys_{357} (before TM 6). Close examination of the mobility of the 24 kDa peptide on SDS−PAGE shows a broad band that could suggest the presence of several polypeptides of various lengths.

Analysis of the trypsin digest of MRP1-variant 574 can be seen in panel D of Figure 6. This digested variant produced three large fragments: 111, 130, and 65 kDa. The 111 and 65 kDa fragments correspond to the same ones indicated above. A faintly visible 130 kDa peptide (not highlighted in the figure) corresponds to a cleavage of MRP1 at the linker domain L0, the second trypsin-sensitive site (*41*). In addition, two other fragments with approximate molecular masses of 18 and 6.5 kDa became visible with a higher trypsin concentration (1:25). The appearance of these fragments correlates with the digestion pattern previously observed with IAARh123-labeled MRP1 (*27*). The 6.5 kDa fragment corresponds to the smallest polypeptide containing the HA epitope (574) between two trypsin sites Ser^{542} and Arg^{593}: ^{542}SAYLSAVGTFTWVCTPFLVALCTFAVYVTIDEN[**HA**]NILDAQTAFVSLALFNILR^{593}. The calculated molecular mass of this polypeptide, including the 10 amino acids of the HA epitope, is 6.9 kDa. The underlined regions represent the predicted TM 10 and 11. The MRP1 HA-variants 653, 938, and 1001 (Figure 7E−G, respectively) produced a 31 kDa proteolytic fragment. This shows that IAAGSH photoaffinity labels a region of MRP1 between MSD1 and MSD2. The predicted molecular weight of the primary sequence from amino acid 653 to 1001 is approximately 38 kDa, indicating that this fragment migrated lower than expected and is represented by the 31 kDa band. A more precise location for IAAGSH labeling in this region was apparent in the highly digested MRP1 variant 938; in addition to the 31 kDa band, 24 and 18 kDa fragments could also be resolved. By comparing the 18 kDa band with MRP1 topology and trypsin cutting sites it was possible to localize IAAGSH photoaffinity labeling of MRP1 to a region after NBD1 but before TM 12 of MSD2. We know that this fragment does not extend into MSD2 because no lysine or arginine residues are located from the start of MSD2 up to position 1001 (position of next MRP1 HA-variant).

The HA epitopes of MRP1-variants 938, 1001, and 1222 (Figures 6F−H, respectively) are located to the C-terminal side of L1. As a result, their digestion pattern did not include the 111 kDa fragment found in the five other variants. Instead, an 85 kDa labeled polypeptide was immunoprecipitated, which correlates to the C-terminal fragment produced from the L1 trypsin sensitive site (*25*, *26*). Digestion of MRP1-variant 938 produced two previously discussed fragments, 130 and 85 kDa, whereas only the 85 kDa peptide was visible in variant 1001. Alternatively, the digestion of MRP1 variant 1222 produced three polypeptides: 85, 41, and 7 kDa. The two smaller polypeptides are unique to

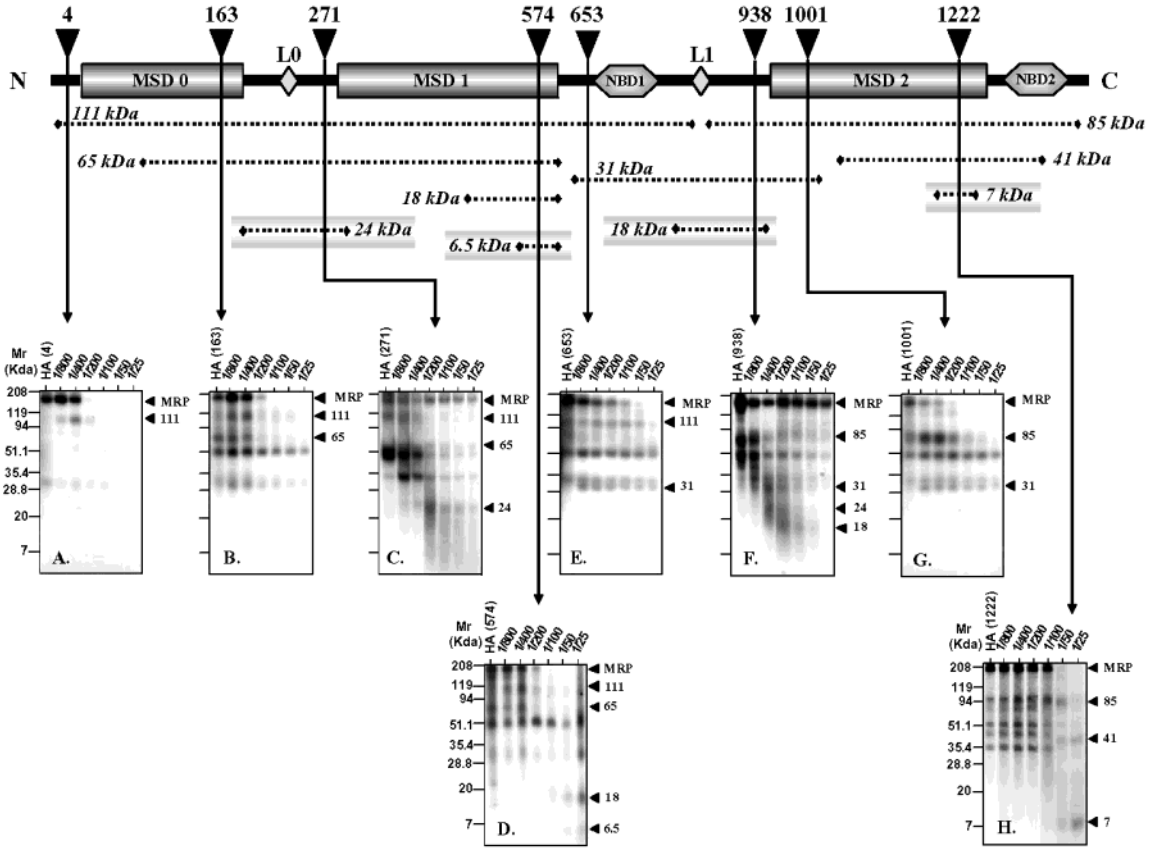

FIGURE 6: Immunoprecipitation of the tryptic digest of IAAGSH-labeled MRP1-HA variants. The image at the top represents the topology of MRP1, and the arrows correspond to the locations of HA epitope insertions. Directly below, in panels A−H, are the resulting labeled and immunoprecipitated peptides derived from the digested plasma membranes containing the eight different full-length MRP1 HA variants. The horizontal dashed lines represent all of the peptides that are resolved by SDS−PAGE on panels A−H. The vertical solid arrows connect the particular MRP1 HA variant in the top panel diagram to its SDS−PAGE digest analysis, and cross horizontal dashed lines representing the peptide fragments are observed in said panel. All plasma membranes were photoaffinity labeled with 4 μM IAAGSH. Each sample was digested with increasing concentrations of trypsin, from 1:800 to 1:25 (w/w: protein/trypsin).

variant 1222. These fragments map IAAGSH photoaffinity labeling to a region at, or near to, the photolabeling site of IAARh123 in MRP1 (*27*). The 7 kDa polypeptide is the smallest photoaffinity labeled fragment that can be immunoprecipitated from the tryptic digest of MRP1-variant 1222. We believe that this band corresponds to the smallest possible trypsin-derived fragment that contains an HA epitope at position 1222 in MRP1. Photoaffinity labeling of the 7 kDa peptide occurs within the following amino acid sequence: ^{1203}LECVGNCIVLFAALFAVISR[**HA-HA**]-HSLSAGLVGLSVSYSLQVTTYLNWLVR^{1249}, in which the underlined regions represent the putative TM 16 and 17. The calculated molecular mass of this polypeptide, including the two HA epitopes, is 7.4 kDa.

In summary, the trypsin digestions shown in Figure 6 indicate that IAAGSH photoaffinity labeled four distinct regions in MRP1. Two of these regions are located within putative transmembrane domains (MSD1 and MSD2) and correspond to TM 10-11 and TM 16-17. These sites are identical to those found for IAARh123. Remarkably, the peptide mapping in Figure 6 also demonstrates that IAAGSH also interacts with two previously unidentified regions corresponding to L0 and L1. These sites are particularly novel because their proposed location is within the cellular cytoplasm.

To confirm the presence of photolabeling sites within the two cytoplasmic regions L0 and L1, similar peptide mapping

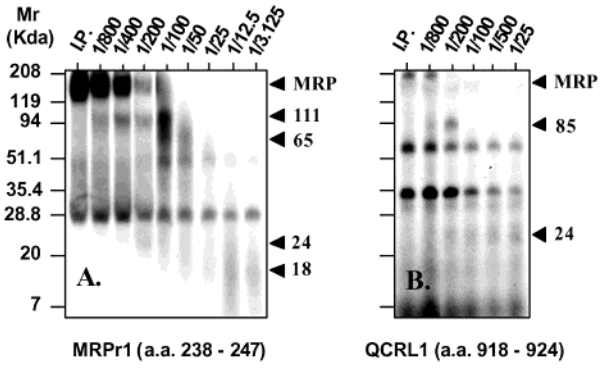

FIGURE 7: Immunoprecipitation of the tryptic digest of IAAGSH-labeled MRP1 with two MRP1-specific mAbs, MRPr1 and QCRL1. The epitopes in MRP1 that are targeted by MRPr1 and QCRL1 are 238−247 and 918−924, respectively. Panels A and B are the resulting labeled and immunoprecipitated peptides derived from the digested plasma membranes of HeLa cells transfected with MRP1 resolved by SDS−PAGE. All plasma membranes were photoaffinity labeled with 4 μM IAAGSH. The samples were digested with increasing concentrations of trypsin from 1:800 to 1:3.125 (w/w: protein/trypsin).

experiments were preformed using two MRP1-specific mAbs (MRPr1 and QCRL1) with epitope sequences located near the HA inserted epitopes of MRP1 variants 271 and 938, respectively (Figure 7). The results obtained from immunoprecipitation with MRPr1 were similar to the MRP1 variant 271. The 111 and 65 kDa products of the L1 trypsin sensitive

site were visible, as well as the smaller 24 kDa peptide (Figure 7A). At higher concentration of trypsin (1:12.5 and 1:3.125, protein/trypsin), an even smaller peptide was visible at approximately 18 kDa. The smearing of the 18 kDa photolabeled peptide is likely due to the presence of many tryptic sites in the L0 domain. Immunoprecipitation of peptides with QCRL1 also confirmed the digestion pattern of MRP1-variant 938 (Figure 7B). The 85 kDa fragment is visible, which is characteristic of MRP1 variants that contain an HA epitope inserted after L1. The smaller 18 kDa band is not visible. The latter is likely due to the loss of the QCRL1 epitope from the photolabeled polypeptides.

It should be pointed out that several IAAGSH-labeled polypeptides were immunoprecipitated, and their bands were visible in the digestion of all eight clones. These polypeptides were located in the undigested sample and did not increase in intensity with increasing concentrations of trypsin and hence are not products of MRP1 digestion. We have determined the approximate size of two nonspecific labeled peptides: 34 and 50 kDa. Previous analysis (*27*) determined that the 50 kDa fragment may originate from the fetal bovine serum used to culture the cell lines. In addition, two photoaffinity labeled polypeptides of the same size are found in undigested HeLa cell plasma membrane (Figure 2).

DISCUSSION

Unlike Pgp1-mediated drug transport, MRP1 activity is often associated with binding or transport of reduced or oxidized glutathione. Several MRP1 substrates are exclusively transported when they are conjugated to GSH (*13*−*15*). Moreover, there is evidence that GSH is co-transported with unmodified drugs such as vincristine (*15*, *16*, *42*). In addition, MRP1 transports GSSG across biological membranes independent of other compounds (*17*). In this study, an iodinated photoreactive analogue of GSH (IAAGSH) was synthesized and used to characterize interactions between GSH and MRP1 and to identify the GSH binding domain(s) in MRP1. Our results show that there is a direct and specific interaction between MRP1 and IAAGSH. Moreover, MRP1 photolabeling by IAAGSH was specifically inhibited with unmodified GSH and to a lesser extent with GSSG and GSH alkyl derivatives. This indicates that the binding characteristics of IAAGSH are very similar to GSH, as compared to GSSG and the alkyl derivatives. The fact that GSSG also caused noticeable competition is expected since it too is a substrate of MRP1 (*43*). We also tested the effect of other known MRP1 substrates on IAAGSH photoaffinity labeling. Surprisingly, both verapamil, and to a lesser extent, vincristine caused an increase in IAAGSH photoaffinity labeling of MRP1. These results are interesting since it was previously demonstrated that verapamil inhibits LTC_4 transport into inside-out MRP1-enriched membrane vesicles by enhancing the transport of GSH (*44*). Vincristine also stimulates ATP-dependent transport of GSH in a similar manner (*15*). Additionally, these studies suggest that verapamil and vincristine mediate GSH transport via a process of co-transport. Our labeling results correlate well with these transport studies and indicate that verapamil and vincristine enhance GSH binding to MRP1 as a preliminary step to co-transport. Conversely, we observed that LTC_4 inhibits IAAGSH photoaffinity labeling. Unlike verapamil and vincristine, LTC_4 is directly conjugated to GSH and is transported independent of free GSH. This indicates that the inhibition of IAAGSH labeling may occur because LTC_4, or its GSH component, competes for the GSH binding site in MRP1, while the increase in GSH photolabeling in the presence of verapamil and vincristine suggests a different or overlapping binding domain(s). Nevertheless, the observed correlation between the photoaffinity labeling results and previous transport studies provides convincing evidence that IAAGSH interacts with the same or similar binding sites as native GSH.

Previous attempts to map the binding site(s) of MRP1 using a quinoline-based drug (IACI) and Rhodamine 123 analogue (IAARh123) identified two binding regions within MRP1: TM 10-11 and TM 16-17 (*27*). This report shows that IAAGSH photolabeled these same regions, in addition to two other sites. The newly identified sites are located in the large cytoplasmic regions on the NH_2-terminal sides of MSD1 and MSD2. The first region (NH_2-terminal half of MRP1) is located in or near to the cytoplasmic region connecting MSD0 to the rest of the protein, designated L0 (∼130 amino acids) (*45*). Several studies attempting to localize binding sites in MRP1 have found L0 to be important. Ren et al. (*29*) used an azido-derivative of the polyhydroxylated sterol acetate (AG-A). They observed that GSH-dependent photoaffinity labeling of the COOH-half of MRP1 requires the L0 domain. They also observed that a double mutation involving tryptophan 261 and lysine 267 within L0 decreases labeling by ∼3-fold (*29*). In addition, Gao et al. showed that a truncated MRP1 mutant lacking MSD0 but still containing L0 behaved like wild-type MRP1 in vesicle uptake and nucleotide trapping experiments (*6*). Similarly, Bakos et al. (*46*) demonstrated that truncated MRP1 lacking MSD0 but retaining the majority of the predicted L0 domain retained considerable LTC_4 transport activity (*46*). Finally, a photoaffinity labeling study using [^{3}H]LTC_4 indicates that all or part of L0 between amino acids 204 and 281 is essential for LTC_4 binding (*28*). Taken together, these observations correlate with the results obtained in this study that show that IAAGSH photolabels a 24 kDa peptide in the MRP1 variant containing an HA epitope at position 271. Furthermore, the use of an MRP1-specific mAb, MRPr1, confirmed this observation by demonstrating that IAAGSH labels MRP1 within the same 24 kDa fragment in addition to a smaller 18 kDa peptide. L0 is found within this 18 kDa region on MRP1, thereby providing convincing evidence that GSH binding does in fact occur within L0. Indeed, this is the first direct demonstration that L0 sequences interact with GSH. A second IAAGSH-labeling region on the COOH-terminal half of MRP1 is located after NBD1 but before TM 12 and contains the L1 region. This labeled portion of MRP1 has a very symmetrical orientation relative to the L0 region. Both binding regions are cytoplasmic and are located on the NH_2-terminal side of a six-pass membrane-spanning domain. Since IAAGSH binds to these regions, while IACI and IAARh123 do not, we suggest that these two cytoplasmic regions form GSH-specific binding sites. They may form autonomous binding sites, or they may act cooperatively to make a binding pocket in the properly folded protein. Cooperative interactions between the NH_2- and COOH-halves of MRP1 are required for high affinity LTC_4 binding (*28*), which favors the possibility that MRP1 contains one GSH-binding pocket comprising the two cytoplasmic

regions. Similarly, the two transmembrane regions that are labeled, TM 10-11 and TM 16-17, may represent a single drug binding pocket that has an affinity for drugs such as IAARh123 and IACI, as well as IAAGSH.

A recent study examined the labeling of MRP1 with a photoactive derivative of GSH, azidophenacyl-GSH (*47*). This study found that the photoactive GSH derivative labels both halves of MRP1. In contrast to our findings, this study found that although L0 is not photolabeled by azidophenacyl-GSH, it is required for binding. Several possibilities may explain these differences. First, perhaps the derivative is modified at the thiol-group of GSH rather than the amino-group, as in IAAGSH. Although azidophenacyl-GSH can substitute functionally for GSH, modification at another group could influence the binding affinity of the compound and/or the spatial orientation of the photoreactive azido moiety relative to the GSH-binding sites. It may also be possible that the peptide comprising amino acids 1−280 of MRP1 is difficult to resolve with a more weakly radioactive [^{35}S] labeled compound. Since this information was not included in that study, it is difficult to compare our findings.

Numerous observations give credence to the existence of a GSH-binding site located in the cytoplasmic portion of MRP1. As a hydrophilic molecule, the pool of cellular GSH is found within the cytoplasm and is thus readily accessible for binding to the cytoplasmic portions of MRP1. Furthermore, we observed that hydrophobic alkyl derivatives with a higher number of hydrocarbon additions (from Met- to Oct-GSH) appear to cause very little inhibition of IAAGSH photoaffinity labeling of MRP1 (Figure 5). This correlates with our observation that the GSH binding site is located within the cytoplasm, in which the alkyl derivatives would not be freely soluble. Conversely, GSH also interacts with the transmembrane drug-binding sites, located in TM 10-11 and 16-17. Despite its polar nature, it is not unusual that GSH can interact with the hydrophobic transmembrane domains because many anionic and polar substrates are known to be substrates of MRP1 (*38*). The interaction of IAAGSH with TM 10-11 and 16-17 is consistent with our findings (data not shown) that increasing concentrations of GSH and GSSG inhibit the photoaffinity labeling of IAARh123 to MRP1, which also occurs within TM 10-11 and 16-17 (*27*). Taken together, we speculate that the four IAAGSH photoaffinity labeled polypeptides represent two GSH binding domains, a cytoplasmic low-affinity and transmembrane high-affinity binding pockets in MRP1. Given its water-soluble nature, GSH is expected to interact with MRP1 cytosolic linker domains (L0 and L1) that participate in or form this low-affinity binding domain. This initial binding could contribute to the dehydration of GSH and subsequent interaction with another, high-affinity binding site, localized to the transmembrane domains. A similar model was proposed earlier by Evers et al. (*48*) to explain GSH-MRP1 interactions. In that model, it was suggested that one site has a high affinity for GSH (G-site) and a low affinity for drugs, while the second site has a high binding affinity for drugs (D-site) and a relatively low affinity for GSH. In the absence of or at low concentrations of drugs, GSH will bind both sites. With the addition of drugs and GSH, both will occupy their preferential site. In the case of high drug concentrations with little or no GSH, the drugs will occupy both sites (*48*). Alternatively, the two GSH binding domains may represent two distinct functions; one is its ability to directly interact with and bind MRP1, and the other is to facilitate the binding of certain MRP1 substrates.

In summary, the findings of this study contribute important information about the interactions between GSH and MRP1, in addition to the value of photoaffinity labeling studies in general. First, IAAGSH behaves in a very similar manner as native GSH. This was initially demonstrated by the ability of IAAGSH to specifically photolabel MRP1. The binding specificity of IAAGSH was further supported by the ability of unmodified GSH to compete and reduce binding of IAAGSH more effectively than other GSH analogues. GSSG, the oxidized glutathione and substrate of MRP1, also produced a noticeable decrease in IAAGSH labeling. In addition, the observation that verapamil and vincristine increased IAAGSH binding presents a strong correlation between GSH binding and its subsequent transport by MRP1. Second, we show that IAAGSH and other MRP1 substrates (IACI and IAARh123) bind to the same sites near TM 10-11 and 16-17. In addition, IAAGSH binds two additional sites located in the cytoplasmic regions on the NH_2-terminal sides of MSD1 and MSD2 (L0 and L1). The L0 site correlates well with previous studies that have implicated this region in GSH binding. These data provide the most precise evidence on the location of GSH binding sites in MRP1. Furthermore, we show that GSH binds and competes for a drug binding site(s), as well as interacting with a GSH-specific site(s), which adds significant insight to our understanding of how MRP1 interacts with anticancer drugs.

REFERENCES

1. Lehnert, M. (1996) *Eur. J. Cancer 32A*, 912−920.
2. Juliano, R. L., and Ling, V. (1976) *Biochim. Biophys. Acta 455*, 152−162.
3. Cole, S. P. C., Bhardwaj, G., Gerlach, J. H., Mackie, C. E., Almquist, K. C., Stewart, A. J., Kurz, E. U., Duncan, A. M. V., and Deeley, R. G. (1992) *Science 258*, 1650−1654.
4. Germann, U. A. (1996) *Eur. J. Cancer 32A*, 927−944.
5. Borst, P., and Schinkel, A. H. (1997) *Trends Genet. 13*, 217−222.
6. Gao, M., Yamazaki, M., Loe, D. W., Westlake, C. J., Grant, C. E., Cole, S. P. C., and Deeley, R. G. (1998) *J. Biol. Chem. 273*, 10733−10740.
7. Hooijberg, J. H., Broxterman, H. J., Kool, M., Assaraf, Y. G., Peters, G. J., Noordhuis, P., Scheper, R. J., Borst, P., Pinedo, H. M., and Jansen, G. (1999) *Cancer Res. 59*, 2532−2535.
8. Cole, S. P. C., Sparks, K. E., Fraser, K., Loe, D. W., Grant, C. E., Wilson, G. M., and Deeley, R. G. (1994) *Cancer Res. 54*, 5902−5910.
9. Jedlitschky, G., Leier, I., Buchholz, U., Barnouin, K., Kurz, G., and Keppler, D. (1996) *Cancer Res. 56*, 988−994.
10. Loe, D. W., Stewart, R. K., Massey, T. E., Deeley, R. G., and Cole, S. P. C. (1997) *Mol. Pharmacol. 51*, 1034−1041.
11. Evers, R., Cnubben, N. H. P., Wijmholds, J., van Deemter, L., van Bladereb, P. J., and Borst, P. (1997) *FEBS Lett. 419*, 112−116.
12. Leier, I., Jedlitschky, G., Buchholz, U., Cole, S. P., Deeley, R. G., and Keppler, D. (1994) *J. Biol. Chem. 269*, 27807−27810.
13. Renes, J., de Vries, E. G. E., Nienhuis, E. F., Jansen, P. L. M., and Muller, M. (1999) *Br. J. Pharmacol. 126*, 681−688.
14. Loe, D. W., Almquist, K. C., Deeley, R. G., and Cole, S. P. C. (1996) *J. Biol. Chem. 271*, 9675−9682.
15. Loe, D. W., Deeley, R. G., and Cole, S. P. C. (1998) *Cancer Res. 58*, 5130−5136.
16. Rappa, G., Lorico, A., Flavell, R. A., and Sartorelli, A. C. (1997) *Cancer Res. 57*, 5232−5237.

17. Leier, I., Jedlitschky, G., Buchholz, U., Center, M., Cole, S. P., Deeley, R. G., and Keppler, D. (1996) *Biochem. J. 314* (*Pt. 2*), 433−437.
18. Clarke, D. M., and Loo, T. W. (1995) *J. Biol. Chem. 270*, 843−848.
19. Rosenberg, M. F., Callagan, R., Ford, R. C., and Higgins, C. F. (1997) *J. Biol. Chem. 272*, 10685−10694.
20. Bakos, E., Hegedus, T., Hollo, Z., Welker, E., Tusnady, G. E., Zaman, G. J. R., Flens, M. J., Varadi, A., and Sarkadi, B. (1996) *J. Biol. Chem. 271*, 12322−12326.
21. Hipfner, D. R., Almquist, K. C., Leslie, E. M., Gerlach, J. H., Grant, C. E., Deeley, R. G., and Cole, S. P. C. (1997) *J. Biol. Chem. 272*, 23623−23630.
22. Vezmar, M., Deady, L. W., Tilley, L., and Georges, E. (1997) *Biochem. Biophys. Res. Commun. 241*, 104−111.
23. Vezmar, M., and Georges, E. (1998) *Biochem. Pharmacol. 56*, 733−742.
24. Vezmar, M., and Georges, E. (2000) *Biochem. Pharmacol. 59*, 1245−1252.
25. Daoud, R., Kast, C., Gros, P., and Georges, E. (2000) *Biochemistry 39*, 15344−15352.
26. Daoud, R., Desneves, J., Deady, L. W., Tilley, L., Scheper, R. J., Gros, P., and Georges, E. (2000) *Biochemistry 39*, 6094−6102.
27. Daoud, R., Julien, M., Gros, P., and Georges, E. (2001) *J. Biol. Chem. 276*, 12324−12330.
28. Qian, Y.-M., Qui, W., Gao, M., Westlake, C. J., Cole, S. P. C., and Deeley, R. G. (2001) *J. Biol. Chem. 276*, 38636−38644.
29. Ren, X. Q., Furukawa, T., Aoki, S., Nakajima, T., Sumizawa, T., Haraguchi, M., Chen, Z. S., Kobayashi, M., and Akiyama, S. (2001) *J. Biol. Chem. 276*, 23197−23206.
30. Meister, A. (1988) *J. Biol. Chem. 263*, 17205−1728.
31. Kast, C., and Gros, P. (1997) *J. Biol. Chem. 272*, 26479−26487.
32. Kast, C., and Gros, P. (1998) *Biochemistry 37*, 2305−2313.
33. Jones, T. R., Zamboni, R., Belley, M., Champion, E., Charlette, L., Ford-Hutchinson, A. W., Frenette, R., Gauthier, J.-Y., Jeger, S., Masson, P., McFarlane, C. S., Piechuta, H., Rokach, J., Williams, H., Young, R. N., DeHaven, R. N., and Pong, S. S. (1989) *Can. J. Physiol. Pharmacol. 67*, 17−28.
34. Lowry, O. H., Rosenberg, N. J., Farr, A. L., and Randall, R. J. (1951) *J. Biol. Chem. 193*, 265−275.
35. Nare, B., Prichard, R. K., and Georges, E. (1994) *Mol. Pharmacol. 45*, 1145−1152.
36. Georges, E., Zhang, J. T., and Ling, V. (1991) *J. Cell. Physiol. 148*, 479−484.
37. Fairbanks, G., Steck, T. L., and Wallach, D. F. (1971) *Biochemistry 10*, 2606−2617.
38. Towbin, H., Staehelin, T., and Gordon, J. (1979) *Proc. Natl. Acad. Sci. U.S.A. 76*, 4350−4354.
39. Bagrij, T., Klokouzas, A., Hladky, S. B., and Barrand, M. A. (2001) *Biochem. Pharmacol. 62*, 199−206.
40. Qian, Y.-M., Song, W.-C., Cui, H., Cole, S. P. C., and Deeley, R. G. (2001) *J. Biol. Chem. 276*, 6404−6411.
41. Hipfner, D. R., Almquist, K. C., Stride, B. D., Deeley, R. G., and Cole, S. P. C. (1996) *Cancer Res. 56*, 3307−3314.
42. Mao, Q., Deeley, R. G., and Cole, S. P. (2000) *J. Biol. Chem. 275*, 34166−34172.
43. Jedlitschky, G., Leier, I., Buchholz, U., Center, M., and Keppler, D. (1994) *Cancer Res. 54*, 4833−4836.
44. Loe, D. W., Deeley, R. G., and Cole, S. P. C. (2000) *J. Pharmacol. Exp. Therap. 293*, 530−538.
45. Hipfner, D. R., Deeley, R. G., and Cole, S. P. (1999) *Biochim. Biophys. Acta 1461*, 359−376.
46. Bakos, E., Evers, R., Szakacs, G., Tusnady, G. E., Welker, E., Szabo, K., de Haas, M., van Deemter, L., Borst, P., Varadi, A., and Sarkadi, B. (1998) *J. Biol. Chem. 273*, 32167−32175.
47. Qian, Y., Grant, C. E., Westlake, C. J., Zhang, D., Lander, P. A., Shepard, R. L., Dantzig, A. H., Cole, S. P. C., and Deeley, R. G. (2002) *J. Biol. Chem. 277*, 35225−35231.
48. Evers, R., de Haas, M., Sparidans, R., Beijnen, J., Wielinga, P. R., Lankelma, J., and Borst, P. (2000) *Br. J. Cancer 83*, 375−383.

BI0268807